Kovove Mater. 54 2016 55–60
DOI: 10.4149/km_2016_1_55

Shear strength and fracture characteristics of the Al_2O_3-TiC/Q235 vacuum diffusion bonded joint

Wanqun Huang[1]*, Yajiang Li[2], Juan Wang[2]

[1] *College of Mechanical & Electronic Engineering, China University of Petroleum (East China), Qingdao 266580, Shandong Province, P. R. China*
[2] *Key Laboratory for Liquid-Solid Structural Evolution and Processing of Materials (Ministry of Education), Shandong University, Jinan 250061, Shandong Province, P. R. China*

Received 9 December 2014, received in revised form 15 January 2015, accepted 22 January 2015

Abstract

Diffusion bonding of composite ceramics Al_2O_3-TiC to low carbon steel Q235 has been carried out by using Ti/Cu/Ti as multi-interlayer. The microstructure and fracture morphology of Al_2O_3-TiC/Q235 diffusion bonded joint were studied via scanning electron microscopy and electron probe microanalysis. The results indicate that an interfacial transition zone was formed between Al_2O_3-TiC and Q235. The Al_2O_3-TiC/Q235 diffusion bonded joints were produced with the shear strength of 111 MPa. As the Al_2O_3-TiC/Q235 joint was subjected to a shear force, only elastic deformation occurred, since the load-displacement curve is a typical brittle fracture curve of the ceramics. It shows that the fracture occurred inside the Al_2O_3-TiC ceramics, and the strength of the interfacial transition zone is higher than that of the Al_2O_3-TiC ceramics. The morphology of the fracture surfaces in the Al_2O_3-TiC ceramics possesses typical features with a mirror region, a mist region, and a hackle region.

K e y w o r d s: ceramic matrix composites (CMC), diffusion bonding, microstructure, shear strength, fracture

1. Introduction

Ceramic matrix composites (CMCs) have drawn much attention, due to their superior properties [1]. The Al_2O_3-TiC CMCs have good application potential in the field such as machinery and metallurgy, etc., due to their high hardness, high wear resistance, high temperature resistance, corrosion resistance and anti-oxidation properties [2, 3]. Because it is difficult to be formed, with the poor toughness and impact resistance, Al_2O_3-TiC CMCs are bonded with the metal materials into the composite components, as one of the effective ways to get better performance. However, it is difficult to obtain the interface with continuous performance between the ceramics and metals. Thermal stress is generated in the ceramic-metal bonded joints, leading to the welding cracks. Therefore, the research into joining of Al_2O_3-TiC CMCs and metal materials is necessary.

This study deals with the joining of Al_2O_3-TiC CMCs to low carbon steel Q235 by using Ti/Cu/Ti as a multi-interlayer. The microstructure, microhardness, shear strength and fracture morphology of the Al_2O_3-TiC/Q235 diffusion bonded joint were analyzed by scanning electron microscope (SEM), micro sclerometer, universal testing machine and electron probe microanalysis (EPMA), to foster the application of Al_2O_3-TiC CMCs.

2. Experimental

This study used hot pressure sintered Al_2O_3-TiC CMCs and low carbon steel Q235. Al_2O_3-TiC ceramics consists of an Al_2O_3 matrix with TiC particles. The chemical composition (wt.%) of Q235 steel is: C 0.14, Si 0.10, Mn 0.5, S 0.035, P 0.035, and Fe balance. The microstructures of Al_2O_3-TiC ceramics and Q235 steel are shown in Fig. 1a and b, respectively. Circular plates of Al_2O_3-TiC ceramics (ø 50 mm × 3 mm) and

*Corresponding author: tel.:+86 0532 86983503-8508; fax: +86 0532 86983300; e-mail address: hwanqun@gmail.com

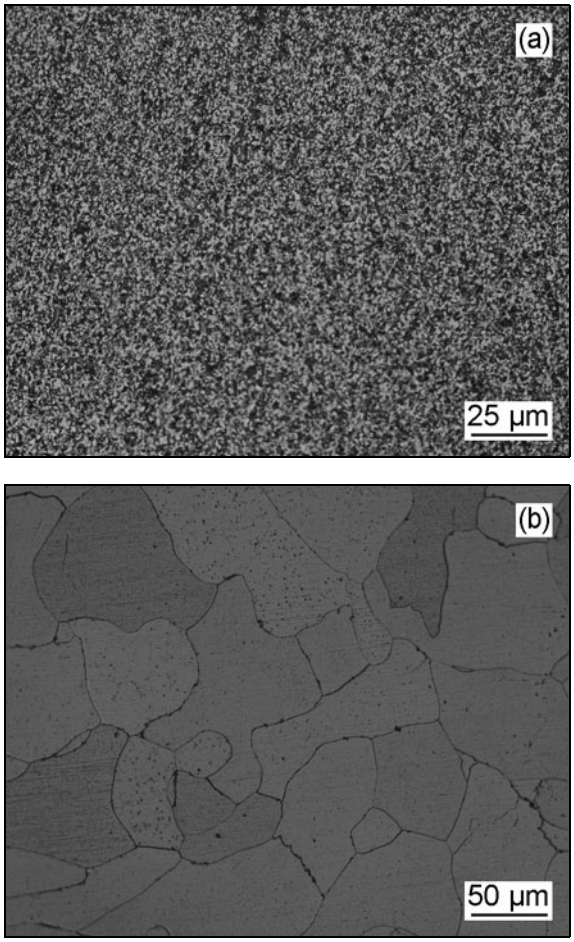

Fig. 1. Microstructures of parent materials: (a) Al_2O_3-TiC CMCs; (b) Q235 steel.

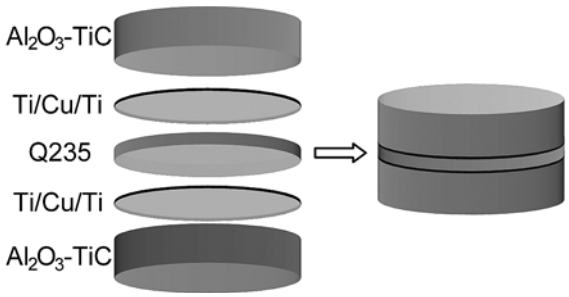

Fig. 2. The schematic diagram of the joint design.

Q235 steel (ø 50 mm × 1.5 mm) were bonded using a Ti/Cu/Ti multi-interlayer. The total thickness of the Ti/Cu/Ti multi-interlayer is 60 μm. The sample configuration is schematically shown in Fig. 2.

The surfaces for bonding were prepared by using of grinding papers of different grades up to 1000 grits, followed by cleaning with acetone in an ultrasonic bath and drying in a warm oven. The joint assembly was performed in a 1×10^{-4} Pa vacuum atmosphere and

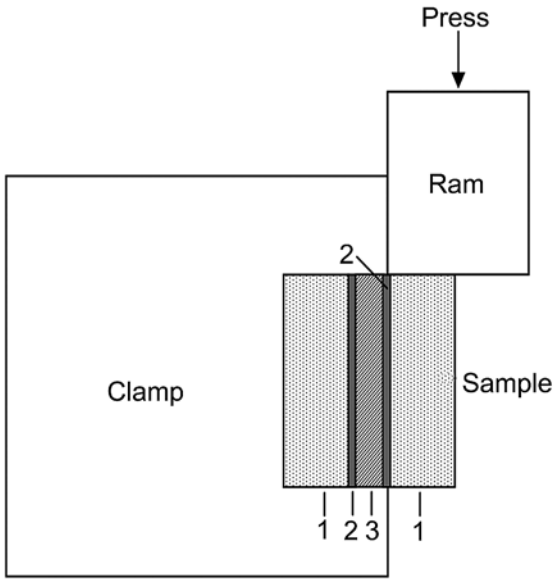

Fig. 3. The schematic setup of the shear strength test for the Al_2O_3-TiC/Q235 joint: 1 – Al_2O_3-TiC; 2 – interlayers; 3 – Q235.

a uniaxial load of 15 MPa was applied to the sample at a bonding temperature of 1180 ℃. At this bonding temperature, joints were prepared at holding time of 45 min. The heating and cooling rates of 15 ℃ min^{-1} were employed during the heating and cooling cycles.

Selected samples were cut, mounted, polished, and etched for microscopic evaluation. The samples were etched with a solution of 5 ml nitric acid in 95 ml ethanol for 5–10 s to reveal the microstructure morphology of the interfacial transition zone in the Al_2O_3--TiC/Q235 joints. After that, a Nikon AFX-IIA metalloscope was used to characterize the joints. A Shimadzu micro sclerometer was used to test the microhardness distributions in the interfacial transition zone. Hardness measurements were conducted using a 100 g of a load with a testing time of 10 s. A WEW--600E universal testing machine was used to test shear strength of the Al_2O_3-TiC/Q235 joints by using a customized fixture. Schematic diagram of the shear strength test for the Al_2O_3-TiC/Q235 joint is shown in Fig. 3. The fractography of the tested samples was analyzed by JXA-8800R electron probe microanalysis (EPMA).

3. Experimental results and analysis

3.1. Microstructure and microhardness

Figure 4a shows the interfacial microstructure in the Al_2O_3-TiC/Q235 diffusion bonded joint. The Al_2O_3-TiC ceramics joins with the Q235 steel closely through the interfacial transition zone. There are no microcracks, voids or unbonded regions existing at or

Table 1. The experimental and calculated results of the shear strength of Al_2O_3-TiC/Q235 interface

Number	Shear area S (mm^2)	Maximum load F_{max} (kN)	Shear strength σ_τ (MPa)	Average shear strength $\bar{\sigma}_\tau$ (MPa)	Fracture locus
1	10 × 10	11.4	114	111	Fractured in the ceramics
2	10 × 10	10.8	108		

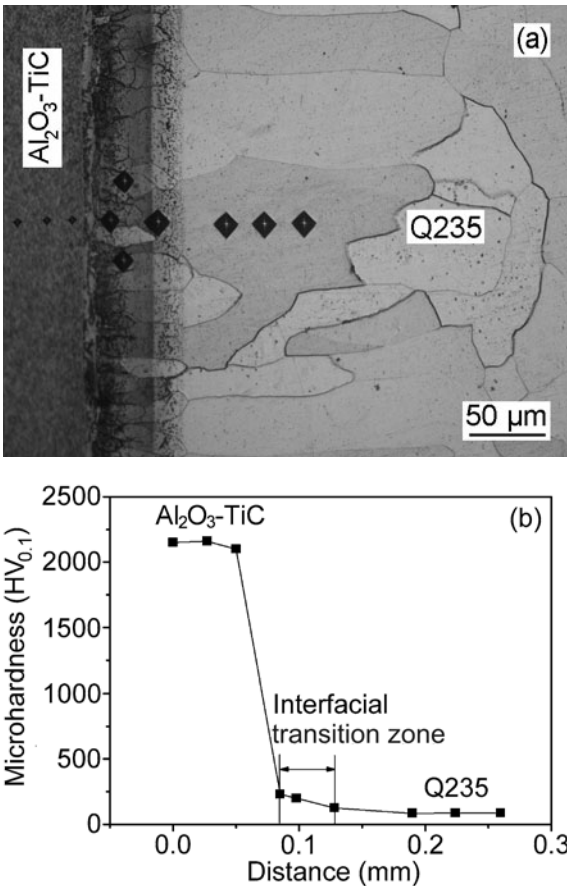

Fig. 4. Microhardness distribution in the Al_2O_3-TiC/Q235 joint: (a) Microstructure and location of measurement; (b) Microhardness distribution.

near the interface. The columnar grains nucleate and grow perpendicular to the interface. Thus, the grains are formed across the interface, which is beneficial to improve the performance of the Al_2O_3-TiC/Q235 joint. The microstructure of the interfacial transition zone is different from the substrates in two sides.

Microhardness near the Al_2O_3-TiC/Q235 interface was measured via the SHIMADZU micro sclerometer with a load of 100 g for 10 s, and the results are shown in Fig. 4b.

It can be seen from Fig. 4b that the microhardness of the interfacial transition zone is far lower than that of Al_2O_3-TiC and slightly higher than that of Q235. It indicates that no brittle phases with higher hardness are formed in the interfacial transition zone. This is beneficial in improving the joint properties.

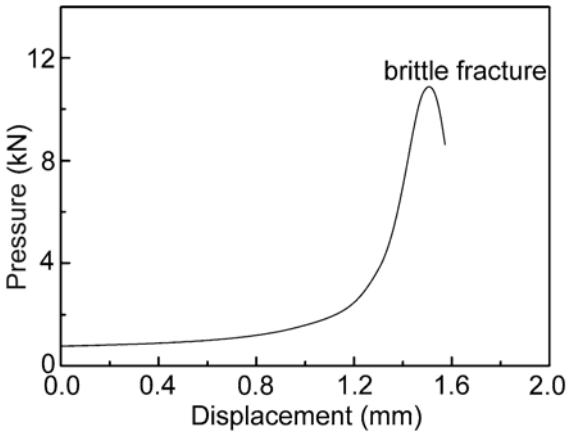

Fig. 5. The load-displacement curve of the Al_2O_3-TiC/Q235 joint in the shear test.

3.2. Shear strength

For the Al_2O_3-TiC/Q235 diffusion bonded joint, two samples were cut from the joint by wire cutting, the sample size was 10 mm × 10 mm × 8.5 mm. After the sample surface had been ground, the shear test was conducted on a hydraulic universal testing machine. The load-displacement curve of the Al_2O_3-TiC/Q235 joint during the shear process is shown in Fig. 5 and the results of shear strength are shown in Table 1.

The Al_2O_3-TiC/Q235 diffusion bonded joints were produced with the average shear strength of 111 MPa (see Table 1). It can be seen from Fig. 5, during the shearing for Al_2O_3-TiC/Q235 diffusion bonded joint, only elastic deformation occurred without yield and plastic deformation. Load-displacement curve is a typical brittle fracture curve of the ceramics before a fracture occurs, load and displacement still keep a good linear relationship, after fracture, the load decreases suddenly.

3.3. Fracture surface analysis

3.3.1. Fracture morphology

The Al_2O_3-TiC/Q235 diffusion bonded joint fractured in the Al_2O_3-TiC ceramics side near the inter-

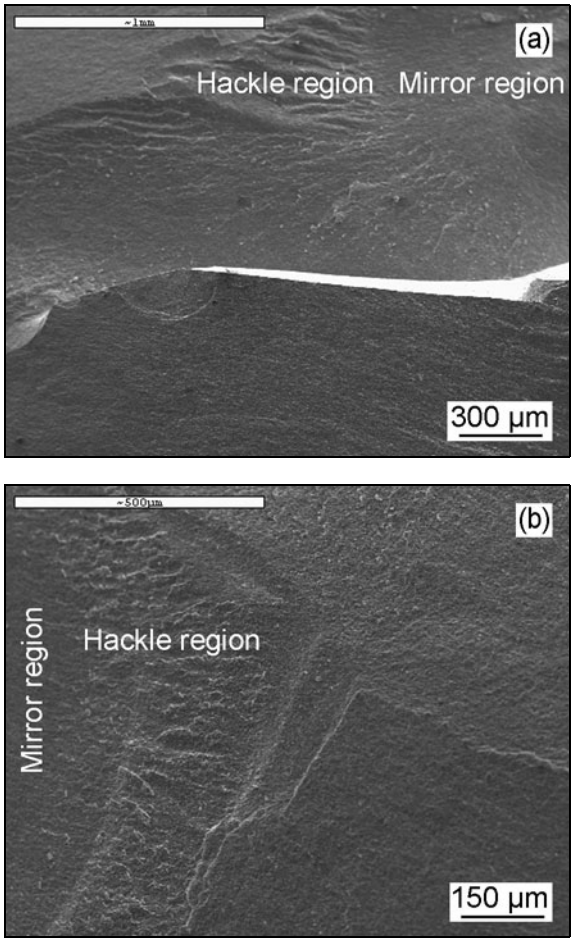

Fig. 6. Shear fracture morphology of the Al_2O_3-TiC/Q235 joint.

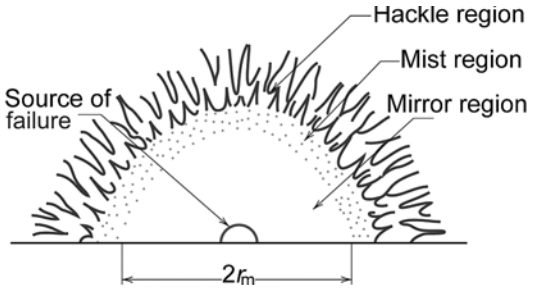

Fig. 7. Schematic illustration of typical features observed on the fracture surface of a brittle ceramics [6].

face. The shear fracture morphology is shown in Fig. 6.

It can be seen in Fig. 6, the morphology of fracture surfaces in the Al_2O_3-TiC ceramics presents some markedly different features from those appearing in metals, and it possesses typical features on the fracture surface of brittle materials. Usually, the failure of ceramics begins at a flaw. After crack nucleates, it propagates slowly at the beginning. As it accelerates, its energy release rate increases, until a critical (or terminal) velocity is achieved. Upon reaching this critical velocity, a crack may branch (or bifurcate). This process may be successively repeated until a family of cracks is produced.

During propagation, a crack interacts with the microstructure of the material, with the stress, as well as with elastic waves that are generated. These interactions produce distinctive features on the fracture surface. Furthermore, these features provide important information on the locus of crack initiation and the source of the crack-producing defect.

Typical features on the fracture surfaces of brittle ceramics are shown in the schematic diagram of Fig. 7. Johnson and Holloway made a systematic exposition of this kind of fracture morphology [4, 5]. The crack surface that is formed during the initial acceleration stage of propagation is flat and smooth and appropriately termed the mirror region (see Fig. 7). For a fracture of glass, this mirror region is extremely flat and highly reflective, on the other hand. For a fracture of polycrystalline ceramics, the flat mirror surfaces are rougher and bear a granular texture. As the crack propagates upon reaching its critical velocity, the crack begins to branch – that is, the crack surface changes propagation direction. At this time, there is a roughening of the crack interface on a microscopic scale, and the arisen region with slightly poor reflectivity is called as a mist region. The mist is a faint annular region just outside the mirror. It is often not discernible for polycrystalline ceramic pieces, particularly for Al_2O_3-TiC ceramic fracture surface. Finally, with the bifurcation of the cracks, the surface of fracture becomes very rough, and the region is formed with striations or lines, called as a hackle region, as noted in Fig. 7.

The hackle is composed of a set of striations or lines that radiate away from the crack initiation site in the direction of crack propagation; furthermore, they intersect near the crack initiation site, and may be used to pinpoint its location. The surface of a hackle region is composed of many facets with a relatively larger area and irregular orientation. These facets are separated by big steps, which keep parallel to the main direction of propagating cracks. Changes of fracture surface appearance are related to increasing of surface roughness. From mirror to mist, and then to hackle, the transformation is associated with a gradual change of roughness. This change of roughness is continuous and related to the variation of crack length.

These features of this type of fracture may be qualitatively analyzed and explained: when the crack nucleates, stress concentration forms at the crack tip. While reaching critical stress, the crack begins to propagate, satisfying the Griffith equation of crack propagation

critical condition as below:

$$\sigma_{\mathrm{f}} = \left(\frac{EG_{\mathrm{c}}}{\pi a}\right)^{1/2}, \tag{1}$$

$$\sigma_{\mathrm{f}} = \left[\frac{EG_{\mathrm{c}}}{\pi(1-\mu^2)a}\right]^{1/2}, \tag{2}$$

where σ_{f} is the fracture stress, G_{c} is the critical energy release rate for crack propagation, μ is Poisson's ratio, E is elastic modulus, and a is the radius of the crack.

Under the constant load, an increase of crack length means that fracture is in an unstable state. Crack propagation is driven by additional energy. From fracture mechanics, once the stress intensity factor K_{I} reaches the fracture toughness K_{IC}, as the crack propagates, K_{I} is much larger than K_{IC}. As the crack propagates with faster speed, the speed of energy release also increases quickly, stress intensity of crack tip during movement is also growing rapidly. Larger stress and more energy release cause the aggravation of micromechanics activity for the crack and gradual increase of roughness for the fracture surface, thus, forming the features of a mirror, mist, and hackle regions. Boundary shape of the mirror, mist, and hackle regions is all approximately circular circle center all situated in crack nucleation, indicating that during accelerated propagation of the crack outwards, the speed in all directions is the same.

When a failure happens with the surface morphology of mirror, mist, and hackle regions, qualitative information regarding the magnitude of the fracture-producing stress is available from the measurement of the mirror radius (see Fig. 7). This radius is a function of the acceleration rate of a newly formed crack – that is, the greater this acceleration rate, the sooner does the crack reach its critical velocity and the smaller the mirror radius. Furthermore, the acceleration rate increases with the stress level. Thus, as the fracture stress level increases, the mirror radius decreases; experimentally it has been observed that

$$\sigma_{\mathrm{f}} = \frac{M}{r_{\mathrm{m}}^{0.5}}, \tag{3}$$

where σ_{f} is the fracture stress, r_{m} is the radius of the mirror region, and M is a constant [7].

As a result, the morphology of the fracture surfaces with mirror, mist and hackle regions is formed under tensile stress [4, 5, 8]. Tensile stress exists during shear testing of the Al_2O_3-TiC/Q235 joint. For example, residual tensile stress easily forms in the ceramics near the interface of Al_2O_3-TiC/Q235 joint. On the other hand, during shearing, there can be a misalignment between two pressure heads, leading to bending of a sample and inducing relevant tensile stress.

Table 2. Composition of fracture surface of the Al_2O_3--TiC/Q235 joint

Elements	Energy spectrum	(wt.%)	(at.%)
O	ED	31.44	55.27
Al	ED	16.71	17.41
Ti	ED	38.37	22.53
Cr	ED	0.42	0.23
Fe	ED	2.21	1.11
Ni	ED	3.61	1.73
Mo	ED	4.40	1.29
W	ED	2.84	0.43

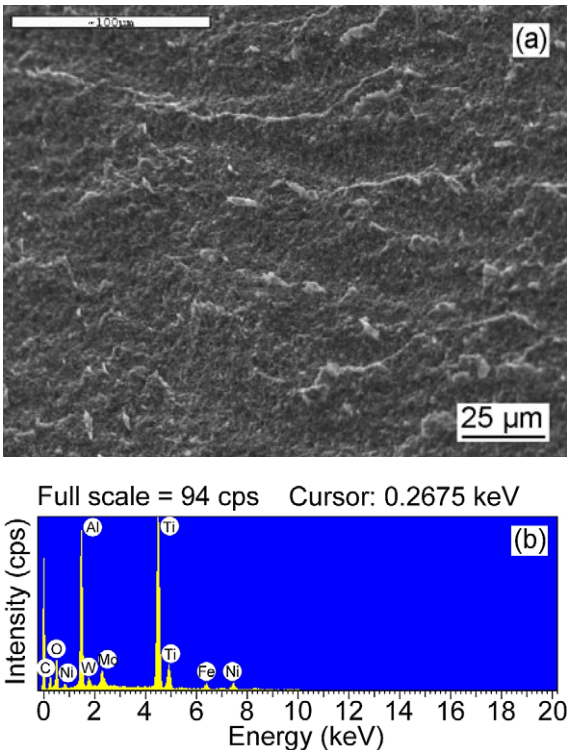

Fig. 8. The composition of the fracture surface.

3.3.2. EDS analysis

Composition analysis was made on the fracture surface of the Al_2O_3-TiC/Q235 joint, the results are shown in Fig. 8 and Table 2.

The results show that the fractured surface mainly contained O, Al, and Ti, as well as some other elements, which all come from the Al_2O_3-TiC base. It indicates that the fracture with mirror, mist, and hackle regions indeed occurs in the Al_2O_3-TiC ceramics, rather than in the interfacial transition zone.

4. Conclusions

1. The Ti/Cu/Ti multi-interlayer is used in dif-

fusion bonding for Al_2O_3-TiC ceramics and Q235 steel. An interfacial transition zone is formed between Al_2O_3-TiC and Q235. The microhardness of the interfacial transition zone is far lower than that of Al_2O_3--TiC and slightly higher than that of Q235, indicating that no brittle phases with higher hardness were formed in the interfacial transition zone.

2. The Al_2O_3-TiC/Q235 diffusion bonded joints were produced with the shear strength of 111 MPa. During the shear test of the Al_2O_3-TiC/Q235 joint, only elastic deformation occurred with no yield and plastic deformation involved, as the load-displacement curve is a typical brittle fracture curve of the ceramics. Also, fracture occurred in the Al_2O_3-TiC ceramics, and the strength of the interfacial transition zone is higher than that of the Al_2O_3-TiC ceramics.

3. The morphology of the fracture surfaces of the Al_2O_3-TiC ceramics possesses typical features with a mirror region, a mist region, and a hackle region. The fracture surfaces mainly contain O, Al, and Ti, supporting that fracture with mirror, mist, and hackle regions indeed occurred in the Al_2O_3-TiC ceramics, and not in the interfacial transition zone.

Acknowledgements

This work was supported by the Fundamental Research Funds for the Central Universities (14CX02076A).

References

[1] Deng, J. X., Cao, T. K., Ding, Z. L., Liu, J. H., Sun, J. L., Zhao, J. L.: J. Eur. Ceram. Soc., *26*, 2006, p. 1317. doi:10.1016/j.jeurceramsoc.2005.02.010

[2] Yin, Z. B., Huang, C. Z., Zou, B., Liu, H. L., Zhu, H. T., Wang, J.: Mater. Sci. Eng. A, *577*, 2013, p. 9. doi:10.1016/j.msea.2013.04.033

[3] Xing, Y. Q., Deng, J. X., Zhao, J., Zhang, G. D., Zhang, K. D.: Int. J. Refract. Met. Hard. Mater., *43*, 2014, p. 46. doi:10.1016/j.ijrmhm.2013.10.019

[4] William, D. C.: Materials Science and Engineering: An Introduction. 7th Edition. New York, John Wiley & Sons, Inc. 2007.

[5] Derek, H.: Fractography: Observing, Measuring and Interpreting Fracture Surface Topography. Cambridge, Cambridge University Press 1999.

[6] Mecholsky, J. J., Rice, R. W., Freiman, S. W.: J. Amer. Ceram. Soc., *57*, 1974, p. 440. doi:10.1111/j.1151-2916.1974.tb11377.x

[7] Shand, E. B.: J. Amer. Ceram. Soc., *42*, 1959, p. 474. doi:10.1111/j.1151-2916.1959.tb13560.x

[8] Zdaniewski, W. A., Conway Jr., J. C., Kirchner, H. P.: J. Amer. Ceram. Soc., *70*, 1987, p. 110. doi:10.1111/j.1151-2916.1987.tb04939.x